A Sensorless Strategy for Speed Control of Axial-Flux Permanent Magnet Motors

Cristian De Angelo[1], Guillermo Bossio[1], Jorge Solsona[2], Guillermo García[1] and María Inés Valla[3]

[1] Grupo de Electrónica Aplicada (GEA), Universidad Nacional de Río Cuarto
Ruta Nacional #36, Km. 601, (X5804BYA) Río Cuarto, Córdoba, Argentina
cdeangelo@ieee.org, gbossio@ing.unrc.edu.ar, g.garcia@ieee.org

[2] Grupo Control Automático y Sistemas (GCAyS), Depto. Electrotecnia, Facultad de Ingeniería
Universidad Nacional del Comahue. Buenos Aires 1400, (8300) Neuquén, Argentina
jsolsona@uncoma.edu.ar

[3] Laboratorio de Electrónica Industrial, Control e Instrumentación (LEICI), Depto. Electrotecnia, Facultad de Ingeniería
Universidad Nacional de La Plata. CC91, (1900) La Plata, Argentina
m.i.valla@ieee.org

***Abstract* — A sensorless strategy for speed control of axial-flux permanent magnet motors is presented. The proposed strategy uses a non-linear reduced order observer that includes information about the waveform of the EMF generated by the motor, which is neither sinusoidal nor trapezoidal. It allows the realization of torque control avoiding position sensor and with minimum torque ripple.**

I. Introduction

Permanent magnet AC machines (PMACMs) are characterized by high performance and high power density, mainly due to the presence of high-energy density magnets.

These machines can be classified as follows [1]:

- Sinusoidal PMACMs (sinusoidal induced EMF);
- Trapezoidal PMACMs (trapezoidal induced EMF).

In both cases, current waveforms and rotor position have to be synchronized in order to control the motor torque.

The use of absolute encoders, resolvers or Hall sensors can make this synchronization possible. However, these sensors increase costs and reduce the drive robustness. It has lead to the investigation and development of different methods of PMACM control avoiding these sensors [2].

Different observers have been proposed for Sinusoidal PMACMs in order to obtain information about the rotor instantaneous position. They allow the generation of sinusoidal currents synchronized with the rotor position in the whole waveform period [3, 4].

On the other hand, constant torque in Trapezoidal PMACMs can be obtained by exciting them with a six-step switched current waveform. These currents only need a good synchronization at each 60°-electrical interval. Thus, the sensorless control algorithm needs to detect only the positions to generate the six-step switched current [5, 6].

However, due to construction, many PMACMs present waveforms that are neither sinusoidal nor trapezoidal. That is the case of axial-flux PMACMs [7]. To obtain constant torque in these cases, currents synchronized with the rotor position must be produced considering the EMF waveform [8].

In the present work, a sensorless strategy using a non-linear reduced order observer that is able to get information from the EMF waveform is proposed. The observer, used with the control strategy proposed in [8], allows the motor torque control (without position sensor), obtaining lower ripple than the obtained with sinusoidal EMF observers.

This work is organized as follows: the PMACM general model is presented first; then, the proposed observer is developed; then, the observer is used in a sensorless speed control strategy. Finally, experimental and simulation results are included and the conclusions are drawn.

II. PMACM Model

The PMACM dynamic model, in a stationary reference frame α–β , can be presented as follows [9]:

$$\begin{cases} \dfrac{di_\alpha}{dt} = \dfrac{-R}{L} i_\alpha - \dfrac{1}{L} e_\alpha + \dfrac{1}{L} v_\alpha \\ \dfrac{di_\beta}{dt} = \dfrac{-R}{L} i_\beta - \dfrac{1}{L} e_\beta + \dfrac{1}{L} v_\beta \end{cases}, \tag{1}$$

$$\begin{cases} \dfrac{d\theta}{dt} = \omega \\ \dfrac{d\omega}{dt} = \dfrac{1}{J} T_e - \dfrac{B}{J} \omega \end{cases}, \tag{2}$$

where i_α, i_β, e_α, e_β, v_α, v_β, represent the current, induced EMF and voltage components respectively, within a stationary reference frame; R and L are the stator resistance and inductance respectively. The variables θ, ω and T_e represent the rotor position and speed and the electromagnetic torque produced by the motor. J and B are inertia and viscosity respectively.

The EMF induced in the stator windings is given by the time derivative of the linked flux, that is:

$$\begin{cases} e_\alpha = \dfrac{d\lambda_\alpha}{dt} = \dfrac{\partial\lambda_\alpha}{\partial\theta}\omega = \varphi_\alpha(\theta)\,\omega \\ e_\beta = \dfrac{d\lambda_\beta}{dt} = \dfrac{\partial\lambda_\beta}{\partial\theta}\omega = \varphi_\beta(\theta)\,\omega \end{cases}, \tag{3}$$

where, λ_α and λ_β are the linked-flux components.

In the sinusoidal PMACM, the flux derivative respect to the rotor position ($\varphi(\theta)$) is a sinusoidal function of the position whereas in trapezoidal PMACMs it is a trapezoidal one. However, in many PMACMs, these functions are neither sinusoidal nor trapezoidal. For this reason, $\varphi(\theta)$ is considered a function to be determined according to the motor type.

III. Nonlinear Observer

In (3), we can observe that the EMF contains the necessary information to determine speed and rotor position, which can be obtained by current and voltage measurements. Thus, it is possible to design an observer to estimate EMF from which speed and rotor position can be obtained. In order to do that, the time derivative of EMF needs to be done, obtaining:

$$\begin{cases} \dfrac{de_\alpha}{dt} = \dfrac{\partial\varphi_\alpha(\theta)}{\partial\theta}\omega^2 + \varphi_\alpha(\theta)\dfrac{d\omega}{dt} \\ \dfrac{de_\beta}{dt} = \dfrac{\partial\varphi_\beta(\theta)}{\partial\theta}\omega^2 + \varphi_\beta(\theta)\dfrac{d\omega}{dt} \end{cases}. \tag{4}$$

From (4), the following EMF observer can be proposed:

$$\begin{cases} \dfrac{d\hat{e}_\alpha}{dt} = \dfrac{\partial\varphi_\alpha(\hat{\theta})}{\partial\hat{\theta}}\hat{\omega}^2 + \varphi_\alpha(\hat{\theta})\dfrac{d\hat{\omega}}{dt} + g\left(L\dfrac{d\hat{i}_\alpha}{dt} - L\dfrac{di_\alpha}{dt}\right) \\ \dfrac{d\hat{e}_\beta}{dt} = \dfrac{\partial\varphi_\beta(\hat{\theta})}{\partial\hat{\theta}}\hat{\omega}^2 + \varphi_\beta(\hat{\theta})\dfrac{d\hat{\omega}}{dt} + g\left(L\dfrac{d\hat{i}_\beta}{dt} - L\dfrac{di_\beta}{dt}\right) \end{cases}, \tag{5}$$

where the time derivatives of stator currents are used as correction terms. An appropriate gain g must be chosen when adjusting the observer in order to obtain exponential convergence as shown in [10].

The estimated current derivatives, necessary for obtaining the correction term, can be obtained from (1),

$$\begin{cases} \dfrac{d\hat{i}_\alpha}{dt} = \dfrac{-R}{L}i_\alpha - \dfrac{1}{L}\hat{e}_\alpha + \dfrac{1}{L}v_\alpha \\ \dfrac{d\hat{i}_\beta}{dt} = \dfrac{-R}{L}i_\beta - \dfrac{1}{L}\hat{e}_\beta + \dfrac{1}{L}v_\beta \end{cases}. \tag{6}$$

Furthermore, the time derivative of speed can be obtained from (2),

$$J\frac{d\hat{\omega}}{dt} = T_e\left(\hat{\theta}, i_\alpha, i_\beta\right) - B\hat{\omega}. \tag{7}$$

If the electromagnetic torque is given by:

$$T_e = \varphi_\alpha i_\alpha + \varphi_\beta i_\beta, \tag{8}$$

then,

$$\frac{d\hat{\omega}}{dt} = \frac{1}{J}\left(\varphi_\alpha(\hat{\theta})\,i_\alpha + \varphi_\beta(\hat{\theta})\,i_\beta\right) - \frac{B}{J}\hat{\omega}. \tag{9}$$

The calculation of the measured current derivative, used in the correction term (5), may end up in a noisy estimation. To avoid that, a variable change can be made:

$$\begin{cases} \hat{\upsilon}_\alpha = \hat{e}_\alpha + g\,L\,i_\alpha \\ \hat{\upsilon}_\beta = \hat{e}_\beta + g\,L\,i_\beta \end{cases}. \tag{10}$$

Making time derivative of (10), and substituting from (5), the proposed observer will result in:

$$\begin{cases} \dfrac{d\hat{\upsilon}_\alpha}{dt} = \dfrac{\partial\varphi_\alpha(\hat{\theta})}{\partial\hat{\theta}}\hat{\omega}^2 + \varphi_\alpha(\hat{\theta})\dfrac{d\hat{\omega}}{dt} + g\,L\dfrac{d\hat{i}_\alpha}{dt} \\ \dfrac{d\hat{\upsilon}_\beta}{dt} = \dfrac{\partial\varphi_\beta(\hat{\theta})}{\partial\hat{\theta}}\hat{\omega}^2 + \varphi_\beta(\hat{\theta})\dfrac{d\hat{\omega}}{dt} + g\,L\dfrac{d\hat{i}_\beta}{dt} \end{cases}. \tag{11}$$

And the estimated EMF can be obtained from (10). Once the estimated EMF is obtained, the speed and rotor position can be calculated by solving (3).

A. Application to the Axial-Flux PMACM

The observer developed in the previous section can be applied to any PMACM. Its implementation only requires knowing the waveform of the flux derivative with respect to the position. This waveform can be experimentally determined previously by measuring instantaneous voltage, rotor position and speed under non-load condition.

In Fig. 1, the waveform of the position derivative of flux (induced EMF divided by speed) is observed. This waveform corresponds to the axial-flux PMACM available at GEA-UNRC laboratory [7], and it was experimentally determined.

To design the observer, the time derivative of the linked flux components are changed to α–β coordinates, within a stationary reference frame, thus allowing to obtain the waveforms shown in Fig. 2.

Fourier series can be used to approximate these waveforms as follows (Fig. 3):

$$\begin{cases} \varphi_\alpha(\theta) = K_e\left(-\sin(P\theta) - \tfrac{1}{25}\sin(5P\theta)\right) \\ \varphi_\beta(\theta) = K_e\left(\cos(P\theta) - \tfrac{1}{25}\cos(5P\theta)\right) \end{cases}, \tag{12}$$

where K_e is the amplitude of the fundamental component and P is the number of pole pairs.

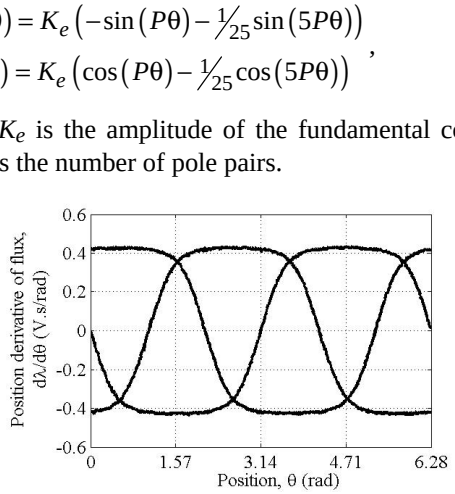

Fig. 1. Position derivative of linked-flux for each phase (electrical radians).

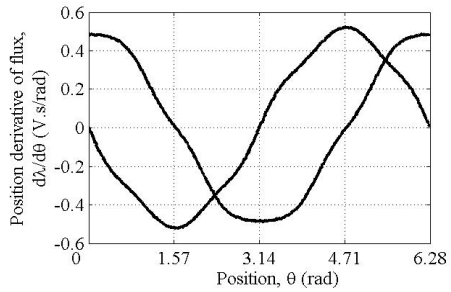

Fig. 2. Position derivative of flux, in α–β coordinates (electrical radians).

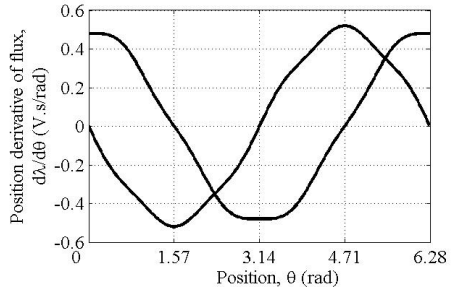

Fig. 3. Approximation of position derivative of flux using Fourier series, in α–β coordinates (electrical radians).

The position derivatives of these functions, necessary to the implementation of (11), are given by:

$$\begin{cases} \dfrac{\partial \varphi_\alpha(\theta)}{\partial \theta} = PK_e\left(-\cos(P\theta) - \frac{1}{5}\cos(5P\theta)\right) \\ \dfrac{\partial \varphi_\beta(\theta)}{\partial \theta} = PK_e\left(-\sin(P\theta) + \frac{1}{5}\sin(5P\theta)\right) \end{cases}. \quad (13)$$

Once the induced EMF is estimated, an inverse function of the expressions (13) should be calculated to obtain the estimated position. However, it is not possible to calculate it exactly, but a good approximation is given by:

$$\hat{\theta} \approx \frac{1}{P}\tan^{-1}\left(\frac{-\hat{e}_\alpha}{\hat{e}_\beta}\right) + \frac{1}{25P}\sin\left(6P\tan^{-1}\left(\frac{-\hat{e}_\alpha}{\hat{e}_\beta}\right)\right). \quad (14)$$

Once the estimated position is obtained, the speed can be calculated, taking into account:

$$\hat{e}_\alpha^2 + \hat{e}_\beta^2 = \hat{\omega}^2\left[\varphi_\alpha^2(\hat{\theta}) + \varphi_\beta^2(\hat{\theta})\right], \quad (15)$$

thus,

$$\hat{\omega} = \sqrt{\frac{\hat{e}_\alpha^2 + \hat{e}_\beta^2}{\varphi_\alpha^2(\hat{\theta}) + \varphi_\beta^2(\hat{\theta})}}. \quad (16)$$

IV. Algorithm for Sensorless Speed Control

Fig. 4 represents a scheme that shows the proposed PMACM drive with sensorless speed control. An internal torque control loop and an external speed control loop constitute the system.

The technique for motor torque control proposed in [8] is used here. According to this technique, the current references to torque control can be obtained by applying the theory of instantaneous reactive power. The active power is the product between the torque reference (T_e^*) and the mechanical speed (ω). The reactive power is made equal zero in order to minimize the stator currents and as a consequence, to reduce torque ripple and copper losses. Therefore, the current references can be expressed as follows:

$$\begin{cases} i_\alpha^* = \dfrac{T_e^*\varphi_\alpha(\theta)}{\varphi_\alpha^2(\theta) + \varphi_\beta^2(\theta)} \\ i_\beta^* = \dfrac{T_e^*\varphi_\beta(\theta)}{\varphi_\alpha^2(\theta) + \varphi_\beta^2(\theta)} \end{cases}. \quad (17)$$

As it can be seen in Fig. 4, the necessary values of φ(θ) and ω to close the control loops are obtained from the proposed observer.

Considering the previously stated equations, the sensorless control algorithm can be implemented as follows:

- Initial conditions: $\hat{\theta}_0, \hat{\omega}_0$.
- Inputs: $i_\alpha, i_\beta, v_\alpha, v_\beta, T_e^*$.
- Algorithm:

$$\begin{cases} \varphi_\alpha(\hat{\theta}) = K_e\left(-\sin(P\hat{\theta}) - \frac{1}{25}\sin(5P\hat{\theta})\right) \\ \varphi_\beta(\hat{\theta}) = K_e\left(\cos(P\hat{\theta}) - \frac{1}{25}\cos(5P\hat{\theta})\right) \end{cases}; \quad (12)$$

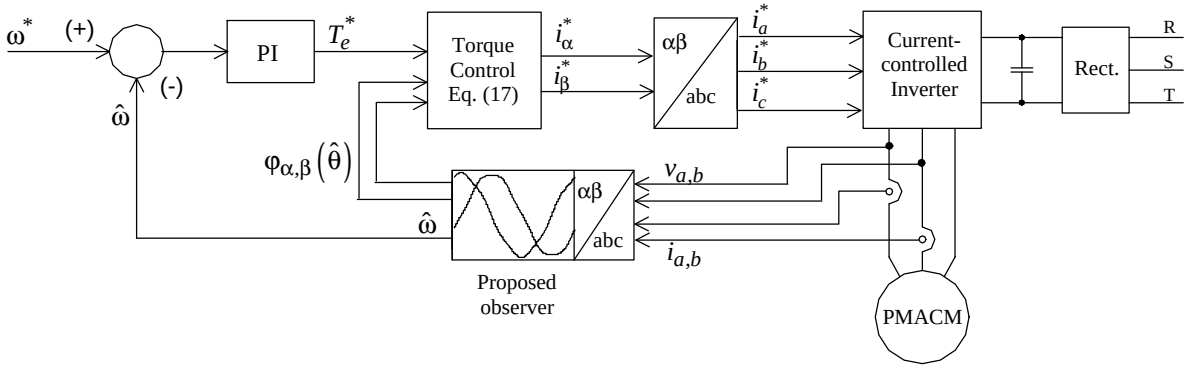

Fig. 4. Position sensorless speed control drive.

$$\frac{d\hat{\omega}}{dt} = \frac{1}{J}\left(\varphi_\alpha\left(\hat{\theta}\right) i_\alpha + \varphi_\beta\left(\hat{\theta}\right) i_\beta\right) - \frac{B}{J}\hat{\omega}\,; \tag{9}$$

$$\begin{cases} \dfrac{d\hat{i}_\alpha}{dt} = \dfrac{-R}{L} i_\alpha - \dfrac{1}{L}\hat{\omega}\,\varphi_\alpha\left(\hat{\theta}\right) + \dfrac{1}{L} v_\alpha \\ \dfrac{d\hat{i}_\beta}{dt} = \dfrac{-R}{L} i_\beta - \dfrac{1}{L}\hat{\omega}\,\varphi_\beta\left(\hat{\theta}\right) + \dfrac{1}{L} v_\beta \end{cases}; \tag{6}$$

$$\begin{cases} \dfrac{d\hat{\upsilon}_\alpha}{dt} = \dfrac{\partial\varphi_\alpha\left(\hat{\theta}\right)}{\partial\hat{\theta}}\hat{\omega}^2 + \varphi_\alpha\left(\hat{\theta}\right)\dfrac{d\hat{\omega}}{dt} + g\,L\dfrac{d\hat{i}_\alpha}{dt} \\ \dfrac{d\hat{\upsilon}_\beta}{dt} = \dfrac{\partial\varphi_\beta\left(\hat{\theta}\right)}{\partial\hat{\theta}}\hat{\omega}^2 + \varphi_\beta\left(\hat{\theta}\right)\dfrac{d\hat{\omega}}{dt} + g\,L\dfrac{d\hat{i}_\beta}{dt} \end{cases}; \tag{11}$$

$$\begin{cases} \hat{e}_\alpha = \hat{\upsilon}_\alpha - g\,L\,i_\alpha \\ \hat{e}_\beta = \hat{\upsilon}_\beta - g\,L\,i_\beta \end{cases}; \tag{18}$$

$$\hat{\theta} \approx \frac{1}{P}\tan^{-1}\left(\frac{-\hat{e}_\alpha}{\hat{e}_\beta}\right) + \frac{1}{25P}\sin\left(6P\tan^{-1}\left(\frac{-\hat{e}_\alpha}{\hat{e}_\beta}\right)\right); \tag{14}$$

$$\hat{\omega} = \sqrt{\frac{\hat{e}_\alpha^2 + \hat{e}_\beta^2}{\varphi_\alpha^2\left(\hat{\theta}\right) + \varphi_\beta^2\left(\hat{\theta}\right)}}\,; \tag{16}$$

$$\begin{cases} i_\alpha^* = \dfrac{T_e^*\varphi_\alpha\left(\hat{\theta}\right)}{\varphi_\alpha^2\left(\hat{\theta}\right) + \varphi_\beta^2\left(\hat{\theta}\right)} \\ i_\beta^* = \dfrac{T_e^*\varphi_\beta\left(\hat{\theta}\right)}{\varphi_\alpha^2\left(\hat{\theta}\right) + \varphi_\beta^2\left(\hat{\theta}\right)} \end{cases}. \tag{17}$$

V. RESULTS

In this section, experimental and simulation results are presented in order to validate the proposed sensorless control strategy. The motor used is an experimental prototype of axial-flux PMACM, available at GEA-UNRC laboratory.

The motor parameters are: *Three-phase axial-flux permanent magnet motor*, 16 poles, 4500 r.p.m., 30 KW.

R = 0.01 Ω,
L = 100 μH,
J = 0.78 Kg m^2,
B = 0.0015 Kg m^2/s.

A. Proposed observer

Experimental results showing how the developed observer works are presented. In these experiments, the measured variables are used to close the control loop.

Fig. 5 shows the actual motor speed and the estimated one by the observer, when a change from 100 to 300 r.p.m. (0.022 to 0.067 p.u.) speed reference is applied to the controller. The estimated speed shows a ripple, which is the result of the noisy measurements. These measurements are being improved for future works.

Fig. 6 shows the unloaded motor speed during start up while running from 0 to 2000 r.p.m. (0.44 p.u.). Here, it can be seen that the ripple in the estimated speed is very small, related to the operating speed.

In Fig. 7, estimated and actual speed during a speed reversal are shown. The speed sign is obtained from the sign of the time derivative of estimated position, since it cannot be obtained from the expression (16). This observer shows the same indistinguishability problems than those that use currents or their derivatives in the correction term [10]. It can be seen that the speed sign cannot be precisely determined at low speed, due to the above mentioned measurement noise.

Finally, Fig. 8 shows the estimation of the position derivative of flux.

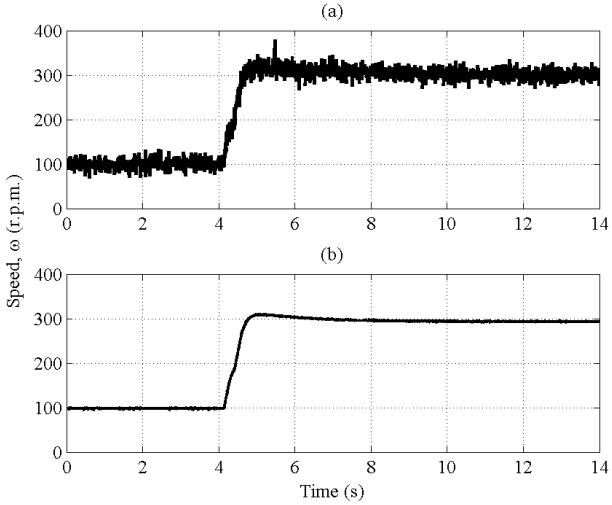

Fig. 5. Estimated speed (a) and actual speed (b).

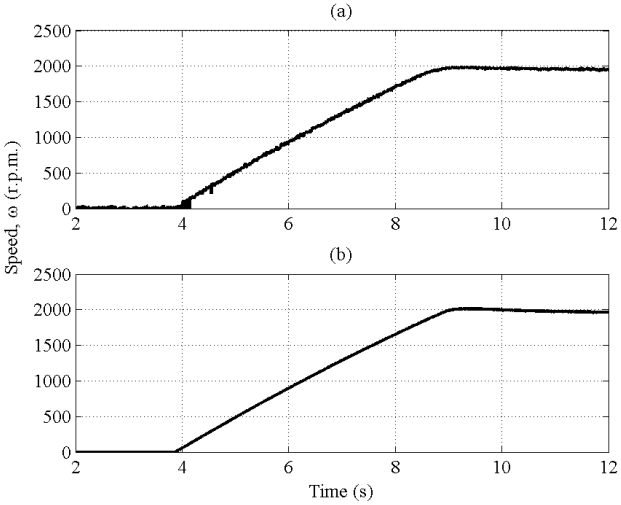

Fig. 6. Estimated speed (a) and actual speed (b).

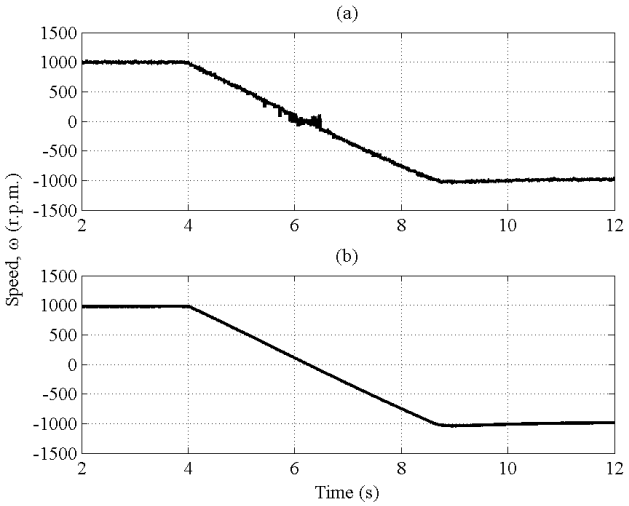

Fig. 7. Estimated speed (a) and actual speed (b) during speed reversal.

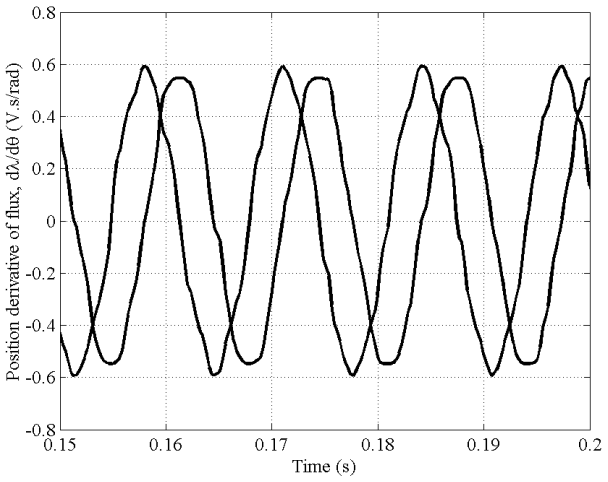

Fig. 8. Estimated position derivative of flux.

B. Position Sensorless Speed Control

The next figures show the results obtained through the simulation of the complete system proposed in Fig. 4. A three-phase voltage source inverter with current control, was modeled in these simulations.

Fig. 9 shows the unloaded motor speed during start up while running from 0 to 4500 r.p.m. (1 p.u.). After 5 sec., the shaft is loaded with constant 65 Nm (1 p.u.). A good response of the closed-loop system is shown in Fig. 10, even under load torque disturbances.

Fig. 11 shows the working system at low speed (225 r.p.m. = 0.05 p.u.). After 1 sec., a constant load of 65 Nm (1 p.u.) is applied. The estimated speed has a ripple due to the harmonics, which has been neglected in (14). This ripple does not depend on the running speed. So it is more visible when the motor runs at very low speed. In order to minimize that effect, the estimated speed that is fed-back has been filtered. This is possible because the ripple is of high frequency.

Finally, Fig. 12 shows the drive response when a change in the sign of the speed reference is applied.

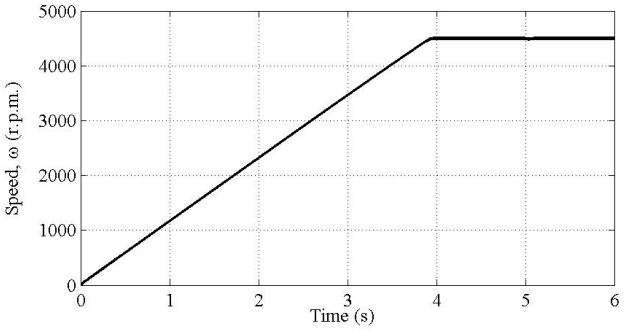

Fig. 9. Control response under high-speed conditions.

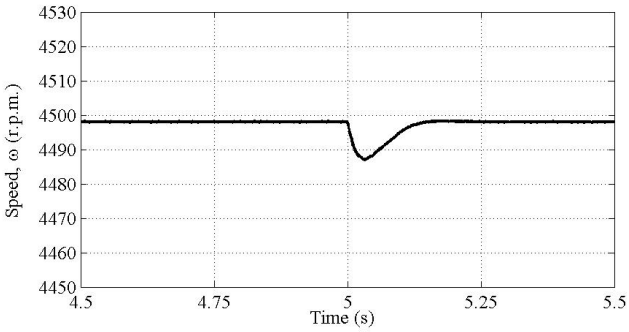

Fig. 10. Control response to a nominal load torque step.

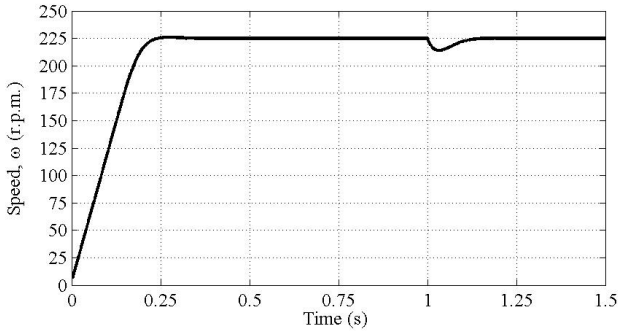

Fig. 11. Control response under low-speed conditions.

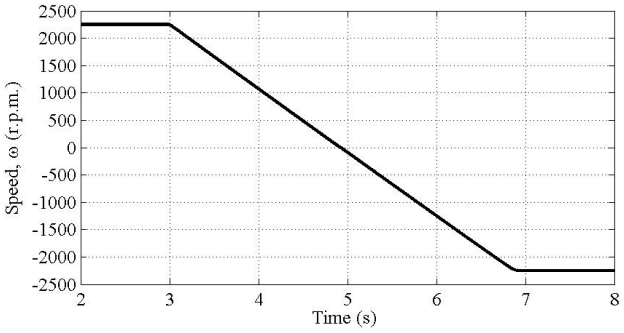

Fig. 12. Speed reversal response.

C. Comparison between the Proposed Observer and a Sinusoidal One.

The control proposed in [8] allows the reduction of the motor torque ripple, provided that the functions $\varphi_\alpha(\theta)$ and $\varphi_\beta(\theta)$ are well known or estimated. The use of the proposed observer greatly improves the torque ripple with respect to a sinusoidal approximation. This is clear in Fig. 13, where the torque produced with both approximations is shown.

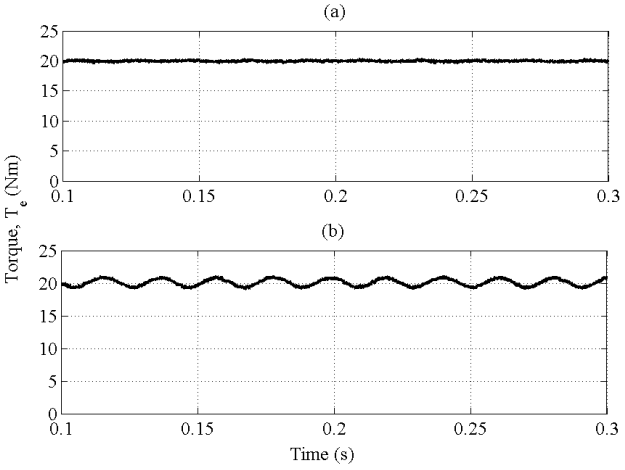

Fig. 13. Torque produced when using the proposed observer (a), and when using a sinusoidal EMF observer (b).

VI. Conclusions

In this work, a sensorless strategy for speed control of axial-flux PMACMs using a non-linear reduced order observer has been presented. The proposed observer includes information about the waveform of the induced EMF, which is neither sinusoidal nor trapezoidal. For the implementation of the observer, it is necessary to know in advance the induced EMF waveform, which is a position function and can be experimentally obtained. The use of the proposed observer together with the torque control proposed in [8], yield to a sensorless motor control obtaining minimum torque ripple and copper losses.

VII. Acknowledgment

The authors wish to acknowledge the financial support and motivation provided by Universidad Nacional de Río Cuarto (UNRC), ANPCyT and CONICET, Argentina.

VIII. References

[1] T. M. Jahns, "Variable Frequency Permanent Magnet AC Machine Drives", in *Power Electronics and Variable Frequency Drives* (Edited by Bimal K. Bose), New York, USA, IEEE Press, 1977, pp. 277-331.

[2] J. Johnson, M. Ehsani and Y. Güzelgünler, "Review of Sensorless Methods for Brushless DC", in *1999 IEEE Industry Applications Conference*, vol. 1, 1999, pp. 143-150.

[3] M. Cendoya, J. Solsona, G. Toccacelli and M. I. Valla, "A Novel Algorithm for Estimating Rotor Position and Speed in Permanent Magnet AC Drives", in *Congresso Brasileiro de Eletrônica de Potência (COBEP '99)*, 1999, pp. 269-273.

[4] Y. Kim and Y. Kook, "High Performance IPMSM Drives without Rotational Position Sensors Using Reduced-Order EKF", *IEEE Transactions on Energy Conversion*, vol. 14, no. 4, pp. 868-873, December 1999.

[5] J. Moreira, "Indirect Sensing for Rotor Flux Position of Permanent Magnet AC Motors Operating in a Wide Speed Range", *IEEE Transactions on Industry Applications*, vol. 32, no. 6, pp. 1394-1403, November/December 1996.

[6] S. Ogasawara, and H. Akagi, "An Approach to Position Sensorless Drive for Brushless DC Motors", *IEEE Transactions on Industry Applications*, vol. 27, no. 5, pp. 928-933, January/February 1991.

[7] A. Agüero, P. Zanello, V. Campra, L. Zanello, C. Candiani, R. Leidhold and G. García, "Accionamiento para Tracción Eléctrica: Motor de Flujo Axial", in *VIII Reunión de Procesamiento de la Información y Control (VIII RPIC)*, Tomo 1, 1999, pp. 89-2 – 95-2.

[8] R. Leidhold, G. García and E. Watanabe, "PMAC Motor Control Strategy, Based on the Instantaneous Active and Reactive Power, for Ripple-Torque and Copper-Losses Minimization", in *Annual Conference of the IEEE Industrial Electronics Society, IEEE IECON 2000*, October 22-28, Nagoya, Japan, 2000.

[9] W. Leonhard, *Control of Electrical Drivers*, Berlin, Springer-Verlag, 1996.

[10] J. Solsona, M. I. Valla and C. Muravchik, "A Nonlinear Reduced Order Observer for Permanent Magnet Synchronous Motors", *IEEE Transactions on Industrial Electronics*, vol. 43, no. 4, pp. 492-497, August 1996.